

## Assessment of Fatigue Failure in FPSO Mooring Systems

Adebanjo Victor Abiola<sup>1</sup>, Ibiba Douglas<sup>1</sup>, Matthew N. O.Sadiku<sup>2</sup>,  
Uwakwe C. Chukwu<sup>3</sup>, Inegiyemiema Morrisson<sup>1</sup>, Onuh Chukwuka Humphery<sup>1</sup>

<sup>1</sup>Center of Excellence in Marine and Offshore Engineering, Rivers State University, Port-Harcourt, Nigeria

<sup>2</sup>Roy G. Perry College of Engineering, Prairie View A&M University, Prairie View, TX, USA

<sup>3</sup>Department of Engineering Technology, South Carolina State University, Orangeburg, SC, USA

### ABSTRACT

Mooring lines failures are a critical subject in FPSO designs, analysis, and operations. This study aims to achieve this by extending damage calculations results from rain flow analysis to the computation of an appropriate range of Weibull parameter  $h$ . The Weibull method is a fatigue analysis method that is done in the frequency domain. Selection of a particular  $h$  parameter that will accurately compute damage is a difficult challenge. So, damage calculations can overestimate or underestimate the fatigue damage and fatigue life of mooring lines. Analysis was also carried out in the frequency domain using Dirlik's method and the results from the two domains compared. Metocean Data for the Gulf of Guinea was obtained and inputted into Orcaflex for analysis. 12 wave classes, current and wind data were extracted and included in a computer model of the FPSO. Rain flow analysis was carried out and the results for all 12 mooring lines in the 12 different wave classes were extracted for analysis. Results from here showed all stresses were within the acceptable limits specified in DNV OS E301 guidelines. Initial analysis was carried out for all 12 wave classes considering Low Frequency (LF) forces alone and another carried out considering Wave Frequency (WF) forces alone for 3 wave classes. The 3 classes selected were in line with DNV Ultimate Limit State (ULS) conditions. Back calculation was used from the fatigue damage results obtained from the analysis and applied to the Weibull equation so an appropriate  $h$  parameter can be gotten. Results obtained can be applied to the fatigue analysis of mooring lines within the Gulf of Guinea environment.

**How to cite this paper:** Adebanjo Victor Abiola | Ibiba Douglas | Matthew N. O.Sadiku | Uwakwe C. Chukwu | Inegiyemiema Morrisson | Onuh Chukwuka Humphery "Assessment of Fatigue Failure in FPSO Mooring Systems" Published in International Journal of Trend in Scientific Research and Development (ijtsrd), ISSN: 2456-6470, Volume-6 | Issue-6, October 2022, pp.1711-1724, URL: [www.ijtsrd.com/papers/ijtsrd52155.pdf](http://www.ijtsrd.com/papers/ijtsrd52155.pdf)



IJTSRD52155

Copyright © 2022 by author (s) and International Journal of Trend in Scientific Research and Development Journal. This is an Open Access article distributed under the terms of the Creative Commons Attribution License (CC BY 4.0) (<http://creativecommons.org/licenses/by/4.0>)



**KEYWORDS:** FPSO, Dirliks method, Weibull Analysis, Fatigue Analysis

### 1. INTRODUCTION

Energy demands are currently projected to increase by as much as 47 percent by the year 2050. Crude oil and natural gas have also been identified as an energy source that would help lead the transition to sustainable energy. With this data, exploration and exploitation of oil and natural gas is expected to increase activities deep offshore as well as the risks associated with such endeavors.

Some of the risks are associated with offshore exploration include the need to ensure that offshore structures are kept at a geographical location, Operation Expenditures (OPEX) costs loss, etc. The actions of waves, tides, currents, and winds on offshore structures cause movements that can be

detrimental to the integrity of the structure. Movements are allowed within a particular offset to ensure that the integrity of subsea assets are maintained. Offsets are set primarily based on the tolerance of the riser that was installed.

Structures used offshore are classified as floating or fixed structures. Floating structures are further classified into four main classes Floating, Production, Storage and Offloading (FPSOs), Semi Submersibles, Surface Piercing Articulated Riser (SPAR) and Offshore Renewable Energy (ORE) structures. Fixed structures on the other hand include Tension Leg Platforms, jack up rigs, etc. The study focuses on FPSOs in the Gulf of Guinea because of its versatility

and reduced Capital Expenditure (CAPEX) in relations to other structures designed to operate in deep water conditions. Also being considered is the need to ensure that there is a dependable framework for fatigue analysis in the Gulf of Guinea. Mooring systems are of two types. They include the temporary and permanent mooring system. The temporary type finds major application in pipe laying vessels, lift vessels, etc. while the latter has more stringent rules since they find application in offshore structures designed to be positioned in a location for long.

Various considerations are infused during the design of the structures. Chief amongst these considerations is the load imposed by the environment. Major contributors include wave, current and wind. Continuous applications of these loads induce various stresses which when continuously applied induces fatigue stresses that are bound to cause failures if not effectively considered during the design stage of the mooring lines. According to Ma et al. (2013) many of these failures have been reported in various offshore sites across the world. Causes of failures vary from improper design, poor quality of mooring line components and poorly trained operators.

With operations regarding exploration moving deep offshore, the industry needs to improve available methods and adequately scrutinize their accuracies on the field. Mooring lines comprises of a top chain, bottom chain, and a rope/ polyester wire. The configurations become trickier as operational depth increases. This is because using a chain all through would be counterproductive when weight increments in relation to the vessel's self-weight is considered. Major mooring accidents have occurred, and the potential impacts become reinforced with the ambitious move towards deep exploration.

Mooring systems are organized in three ways which include: taut mooring; catenary mooring and catenary mooring with buoyancy elements. Some of the features of a mooring line are:

1. Taut mooring made up of chain-synthetic fiber ropes/polyester-chain
2. Catenary mooring made up of chain-steel rope-chain
3. Catenary mooring with buoyancy elements made up of chain-steel wire rope-buoy-steel wire rope-chain.

With increasing leap and movement towards deep water exploration catenary systems are more unpopular and inapplicable due to the increasing weight. Taut leg mooring was developed as a solution to this challenge. In the taut system the seabed is approached horizontally at an angle. The arrangement ensures the ability of the system to resist both horizontal and vertical forces. Catenary systems address horizontal forces alone which is contributed by the weight of the mooring lines.

Larsen (2014) gave a vivid description as shown in the figure below: 1 represents taut mooring, 2 represents catenary system and 3 represents catenary mooring with buoyancy elements. Some of the features incorporated into various mooring systems include anchor, chain synthetic fiber ropes, buoys, clump weights etc.

For chains, their configurations may be stud less or stud link. For chains that must be rearranged several times during their deployment. The weights of the chains are heavy and more likely to be subjected to a great deal of fatigue damage when they are related to others. Larsen (2014) did a comparative study of the properties of the materials used in mooring lines. It is shown in the table 1 below

**Table 1: Properties of some mooring lines**

Material	Diameter (mm)	Weight in air (kg/m)	Weight in water (kg/m)	Typical Axial Stiffness*10 <sup>-5</sup> (KN)
Stud R4 chain	102	230	200	7
Spiral Strand Steel	108	57	48	9
Polyester	175	23	5.9	1.0-4.5

For steel wire ropes several spiral strands which may be covered or uncovered by a plastic sheet are commonly found on most. They are not as heavy as chains and are known to have good fatigue properties consequently making them less of a concern. In shallow waters, they are known to have small fatigue capacity at shallow depths.

For synthetic ropes polyester is one of the most used materials but other high-tech fibers are also deployed. These ropes are known to have less weight but are highly elastic. Ascertaining Fatigue Limit States (FLS) require intricate analysis that are known to be time consuming.

Getting a good grip of the safety requirements of offshore structures makes fatigue an important subject. Its classification is based majorly on how they occur and may vary from mechanical, creep, thermo-mechanical,

corrosion and fretting fatigue. Berge (2006) emphasized that the constantly occurring loads which are lesser than the material yield strength accumulates and lead to material failure.

Fatigue cracks are known to spread and lead to failures in three different modes which are tension, shear and torsion. Besides the aforementioned, In-plane Bending (IPB) and Out of Plane Bending (OPB) is a major contributor to fatigue failure in mooring lines. Yooil et al (2018) carried out an investigation on this concept by combining both hydrodynamic and stress analysis methods. Hydrodynamic analysis was done using the decoupled analysis method and the stress analysis method involved the use of non-linear finite element analysis method.

Rampi et al (2016) employed a multi-axial approach by carrying out a fatigue test with a full-scale chain model. A Finite Element Method (FEM) analysis was also carried out before result comparison. They recommended the use of the multi axial fatigue criterion as opposed to the uniaxial maximum principal stress criterion.

Kim and Kim (2017) evaluated parametrically the stiffness and stress concentration factor which is introduced by IPB and OPB elements. A sensitivity analysis was also conducted on the result to ascertain the significance of the impacts of the numerical friction model.

Fatigue computations are done using a Time Domain (time domain) or Frequency Domain (FD) analysis. Wave loading is known to make results from the results below very uncertain Uncertainty here is made pronounced by the drag forces though wave modelling of waves occurring near the sea surface and current is weighty.

Probabilistic/stochastic Frequency Domain (FD) analysis makes it possible to evaluate damage due to fatigue using two approaches that involves application of stress spectrum that exist in a cross section of the object being subjected to test. The methods include:

- Gaussian methods which are seen as a narrow-banded process that involves the application of Rayleigh distribution computation approach on ranges of peaks and stress.
- Fast Fourier Transform (FFT) application on stress spectrum to generate a stress history that results in a broad banded Gaussian process. Stress history generated is used to compute fatigue damage by cycle and range counting. From this process, the total fatigue damage results are obtained.
- Time domain (TD) analysis is also approached in two ways, and they include:
- Carrying out a rain flow counting analysis which is known to produce results in record time as it uses not so much computation resources.
- Probability distribution selection that is used to estimate parameters based on load history which can be used to calculate fatigue damage by integrating the Probability Density Function (PDF) and the S-N curve.

TD and FD methods can be further broken down into various methods. FD methods include Simple Summation (SS) approach, Combined spectrum method, Dual Narrow Band (DNB). For TD, methods used include Weibull and the Rainfall Analysis Method. Weibull analysis is based on the closed fatigue life equation and an assumption that a hypothetical structure has stress cycles that are stochastic and have a Probability Distribution Function (PDF). Besides the aforementioned, spectral (also frequency) methods such as the Dirlik's approach are used. Propounded in 1985, it aims to estimate the Probability Density Function (PDF) of specific stresses from Power Spectral Density (PSD) obtained from the frequency response of a system. Moments are calculated and used to calculate the damage of a system. Pankaj (2017) applied Dirlik's method to the computation of fatigue stresses in tubular structures, verifying the accuracy of the method in the process. It is known to be more accurate when compared to the Rainflow counting method.

## 2. METHODOLOGY

The field used for the study is located about 120 km off the coast of the South-Eastern region of Niger Delta with coordinates 4.5569°N and 4.6169°E. Metocean conditions in this region are mild and are a function of its position relative to the Inter-Tropical Convergence Zone (ITCZ). Conditions in this region vary from periods with light winds, afternoon rain showers, periods of short-lived intense rainfall, and relatively low wave heights. Metocean data for wind, waves and currents were used for the analysis.

Data used for this thesis was obtained from the Marine Copernicus data repository for metocean data and the downloaded file opened using MATLAB. Geographical coordinates were used to extract the data for the analysis. The wave classes used for the study is shown in the table below.

**Table 2: Wave classes for analysis**

S/N	Direction	Hs(m)	Tz(s)
1	180	3.42	12.72
2	230	3.42	17.60
3	230	2.77	19.47
4	230	2.77	9.70
5	190	3.19	10.60
6	190	3.55	7.30
7	166	3.85	12.00
8	220	4.09	12.00
9	220	2.32	15.60
10	215	2.07	15.90
11	230	1.76	14.00
12	185	2.90	16.90

The Guinean current flows along the coast of West Africa in a direction between 2- and 5-degree North. (Djakoure et al., 2017) A surface speed of 2.13 m/s and a seabed speed of 0.19 m/s was used for the analysis. Orcaflex computes current profiles using the interpolated or the power law method. The power law method was used.

### 2.1. Vessel Description

The FPSO used a case study is installed off the coast of Nigeria and operates in waters that are about 1000m deep. It is spread moored with 12 mooring lines and has a heading of 180 degree in Southwestern direction to reduce the effect of waves on vessel stability. Configuration of mooring lines include a studless top chain, multistrand wire rope and a studless bottom chain. About 1 mile from the FPSO is a Single Point Mooring (SPM) buoy for the offtake of crude produced from the field. A summary of the mooring chain lengths and vessel properties are shown in the tables 3.2 and 3.3 below.

**Table 3: Vessel Parameters (Chanhoe et al., 2016)**

Parameters	Value
Length (m)	305.1
Breadth (m)	58
Depth (m)	21.2
Summer DWT (Tonnes)	350,000 tonnes

**Table 4: Table of mooring line segments length**

S/N	Mooring Chain	Section	Diameter (m)	Section Length(m)
1	Portside line 1-6	Top Chain	0.178	101.20
		Wire Rope	0.098	1103.00
		Bottom Chain	0.178	669.60
2	Starboard Line 1-3	Top Chain	0.178	96.20
		Wire Rope	0.098	1133.60
		Bottom Chain	0.178	644.50
3	Starboard 4-6	Top Chain	0.178	96.00
		Wire Rope	0.098	1101.50
		Bottom Chain	0.178	674.50

### 2.2. Simulation in Orcaflex

Dynamic analysis builds on the positional outcome obtained from the static analysis of a model. It simulates the motion of the model over an appropriate period taking into cognizance the metocean data inputted, the Response Amplitude Operator (RAO), vessel headings, draught and other factors.

A build-up stage precedes dynamic simulation during which motions that encompass low frequency (LF) and Wave Frequency (WF) are slowly revved up from zero to their full size. Currents which are a component of LF motions can be left out of the whole ramping up operations to cut down on transients generated by the switch from static to dynamic analysis.



The unit of time in the software is seconds and wave time origins can be set when inputting wave data. When set to zero (as used in the simulations) wave effects application starts at global time 0 at the end of the revving up stage. Other entries besides 0 which consequently time shifts the wave application time. When several waves are applied, time origins can be spread apart so simulation stages can be spread out.

Model in Orcaflex includes 12 mooring lines, FPSO and a SPM buoy. Risers, water injector pipes, gas export lines, etc. have all been removed to optimize model and reduce simulation runtime. Model used is shown figure 1 below.

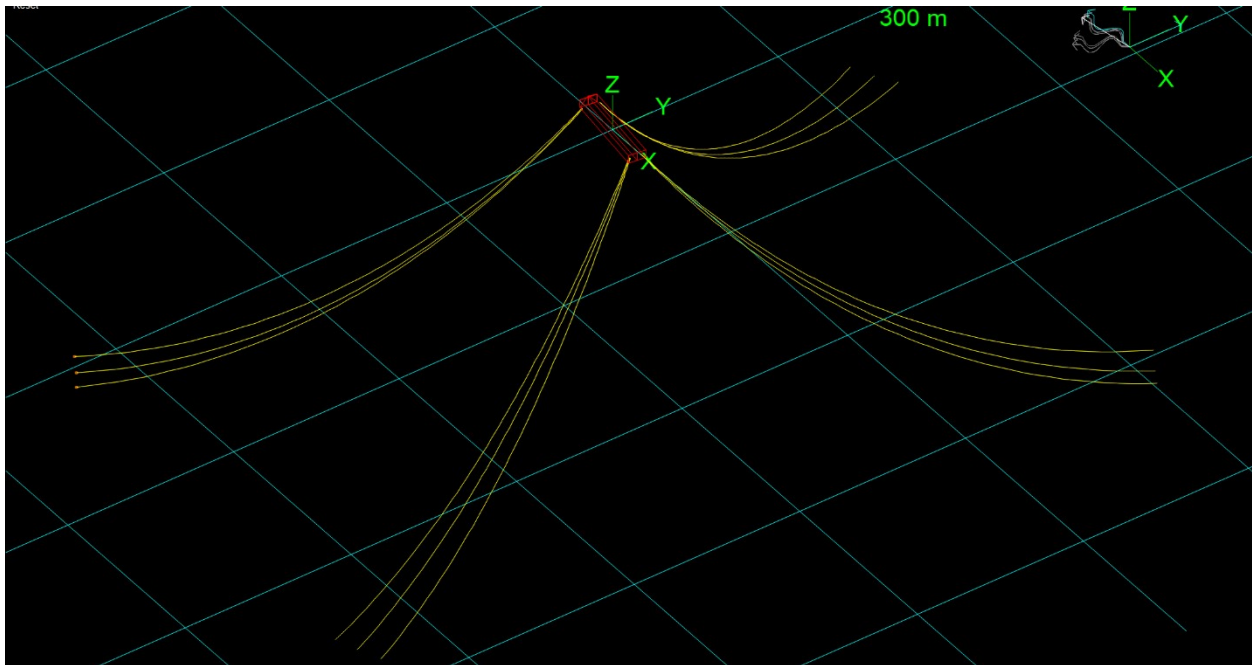


**Figure 1: FPSO Model in Orcaflex**

As part of efforts to Quality Check (QC) the model, attention was given to the grade/type, diameters, and breaking load values of the mooring line components. This was specified and checked using the line type wizard and its data repository for the breaking load. Identifying and making adequate checks in this area also helps select appropriate values (m and k) for the TN curve used for rainflow analysis after loading the simulation files. DNV recommends the following values. Breaking strength is also added for emphasis.

**Table 5: DNV recommended values used for fatigue analysis**

Chain/Rope Type	m	k	Breaking Strength(KN)
Stud less Chain (R4)	3	316	25480
Spiral Strand Wire Rope	4	1000	8000

Low and wave frequency components were also accounted for according to DNV guidelines. The software allows the user to account for these components in simulation runs or both. When running a model using both options a threshold frequency must be set. One thing to be observed was to select the right effects that were applicable to wave or low frequency responses. The possible options include applied loads, wave loads, wave drift load, wave drift damping, sum frequency load, added mass damping, maneuvering load, other damping, current load and wind load. Setting the primary motion to either low, wave or both automatically selects the appropriate primary effects to be used for the runs when all effects are included regardless of any option selected that is not applicable to the primary motion selected. Results were loaded on conclusion of simulation to obtain stress, tension, zero crossing period, etc. from the simulation files for use in Weibull computation and analysis.

### 2.3. Weibull Analysis Case Study

This section assesses how computations are carried out using Wave 1 as an instance on how computations were carried out. Wave 1 simulation files for LF and WF primary motions were used to extract important data used for computations for mooring line P1. It is important to note that all forces and stresses induced in line P1 were checked to ensure that it is safely within the breaking loads of the line components. The extreme statistics option in the software helped predict the maximum tension in line P1 during a 3-hour storm. Prediction results showed a 95 percent confidence limits and showed the effective tension is 9664.68KN. The table below shows other values extracted using the linked statistics and result summary options in the software.

**Table 6: Parameters List Obtained from dynamic simulation results in Orcaflex**

S/N	Variable Name	Value
1	Standard deviation of Low frequency stress component ( $\sigma_l$ )	12934.9415 KN
2	Standard deviation of Wave frequency stress component ( $\sigma_w$ )	11027.2651KN
3	Mean up Crossing Period Tz (s) for the stress component in LF motions	0.1863 sec
4	Mean up Crossing Period Tz (s) for the stress component in WF motions	0.1914 sec
5	Most probable maximum tension ( $\sigma_{mpm}$ )	11,9583 KPa
6	Mean stress ( $\sigma_{mean}$ )	55350.479 KPa

The Weibull Expression used for the calculations is shown below.

$$D = \frac{n_0}{a_D} \cdot \frac{(\Delta\sigma_0)^m}{(m n_0)^{\frac{m}{h}}} \cdot \Gamma\left(\frac{m}{h} + 1\right) \quad 3.6$$

Where,  $\Gamma$  is the gamma function

$\Delta\sigma_0$  is the maximum stress range of  $n_0$  stress cycles

$n_0$  is the total number of stress cycles

m is the negative inverse slope of the SN curve

$a_D$  is the antilog of the intercept of the Log N axis of the SN-curve

h is the Weibull parameter

D is the damage per year

To compute the normalized variance  $\lambda$  of LF and WF motions, the expressions below are used:

$$\lambda_l = \frac{\sigma_l^2}{\sigma_l^2 + \sigma_w^2} \quad (1)$$

$$\lambda_w = \frac{\sigma_w^2}{\sigma_l^2 + \sigma_w^2} \quad (2)$$

For  $\lambda_l$

$$\begin{aligned} \lambda_l &= \frac{12934.9415^2}{12934.9415^2 + 11027.2651^2} \\ \lambda_l &= \frac{167312711.608}{167312711.608 + 121600575.5856} \\ &= \frac{167312711.608}{288913286.8456} \\ &= 0.5791 \end{aligned}$$

For  $\lambda_w$

$$\begin{aligned} \lambda_l &= \frac{11027.2651^2}{12934.9415^2 + 11027.2651^2} \\ \lambda_l &= \frac{121600575.5856}{167312711.608 + 121600575.5856} \\ \lambda_l &= \frac{121600575.5856}{288913286.8456} \\ &= 0.4209 \end{aligned}$$

Since frequency is the inverse of period, the zero up crossing frequencies for LF and WF motions is calculated below.

$$v_l = \frac{1}{0.1863} = 5.366 \text{ Hz}$$

For  $v_l$ ,

$$v_1 = \frac{1}{0.1914} = 5.225 \text{ Hz}$$

To calculate the up-crossing rate through the mean value of the stress spectrum for the combined process, the expression below is used.

$$v_p = \sqrt{\lambda_1^2 v_1^2 + \lambda_1 \lambda_w v_w^2 \delta_w^2} \quad (3)$$

Where  $\delta_w$  is the bandwidth parameter taken as 0.1 according to DNV guidelines.

$$\begin{aligned} v_p &= \sqrt{(0.5791^2 * 5.3677^2) + (0.5791 * 0.4209 * 0.1^2 * 5.225^2)} \\ &= \sqrt{9.6624 + 0.0665} \\ &= \sqrt{9.7289} \\ &= 3.119 \text{ Hz} \end{aligned}$$

To compute the total number of stress cycles  $n_0$ , the expression below is used.

$$n_0 = v_p * T_{1\text{-year}} \quad (4)$$

Where  $T_{1\text{-year}}$  represents the total time in seconds the wave phenomenon lasts for 1 year. An assumption is made here that the wave occurs once a day for 12.72 seconds.

$$\begin{aligned} n_0 &= 3.119 * 365 * 12.72 \\ &= 14480.8932 \text{ cycles} \end{aligned}$$

Maximum stress range ( $\Delta\sigma_0$ ) is computed using the formula below.

$$\begin{aligned} \Delta\sigma_0 &= (\sigma_{\text{mpm}} - \sigma_{\text{mean}}) * 2 \\ &= (119583.9003 - 55350.474) * 2 \\ &= 128,376.8429 \text{ Kpa} \end{aligned} \quad (5)$$

The damage D is computed using the values obtained from the rainflow fatigue analysis carried out in the software. The wire rope section here is used for computation. The values gotten from the simulation is shown in the table 3.6 below.

**Table 7: Damage parameters obtained from software**

Section length	Total Damage Per day	Damage Per year
1103m	6.3286E-09	2.3099e-06

DNVGL-OS-E301 recommends a value for m and  $a_D$  as shown in the table below. This also applies to different line components.

**Table 8: DNV recommended values for SN curve**

Line Component	$a_D$	m
Studless chain	$6.0 * 10^{10}$	3.0
Spiral Rope	$1.7 * 10^{17}$	4.8

On substitution of all parameters into the Weibull equation, the expression can be written as

$$2.3099\text{e} - 06 = \frac{14480.8932}{1.7 * 10^{17}} \cdot \frac{(128.376)^{4.8}}{(\ln 14480.8932)^{\frac{4.8}{h}}} \cdot \Gamma\left(\frac{4.8}{h} + 1\right)$$

A MATLAB code is used to solve this. From results generated from the m file run, the values of h varies from 0.8869 to 0.900 suggesting that the answers are well within acceptable range of h values. The method shown above is then repeated for three wave classes and all mooring lines.

## 2.4. Fatigue Damage in Frequency Domain (Dirlik Method)

To compute fatigue in frequency domain a Power Spectral Density (PSD) diagram of the load is an important aspect. It gives information about the magnitude of a normalized power in frequency domain. Fourier transform (f(w)) is obtained from a time series using the equations below:

$$f(\omega) = \frac{1}{2\pi} \int_{-\infty}^{\infty} f(t) e^{-i\omega t} dt \quad (6)$$

$$PSD = \frac{f(\omega)^2}{\omega} \quad (7)$$

Where  $\omega$  is the frequency in Hz and  $t$  is the total time.

The unit of PSD is  $\text{unit}^2/\text{Hz}$  and is obtained from MATLAB using the `pwelch` command. The stress time history obtained from dynamic simulation carried out in Orcaflex. Data extracted does not include the buildup stage in Orcaflex since the stage 1 simulation is the most important in this case. Tension cycles vary depending on the node being studied. In order to deal with this, data from nodes at regular intervals are extracted and their corresponding PSDs plotted in MATLAB for use in Dirlik's formula.

PSDs obtained from the tension cycles also had their corresponding data plots extracted and put in an excel file. Entries run as high as 16386 for the  $x$  and  $y$  axes respectively. From these values the moments of the curve are computed and applied for use based on Dirlik's method. The expressions used are shown in subsequent sections.

To calculate moments  $m_0, m_1, m_2$  and  $m_4$ , the expression below is used

$$\int f^n G(f) df \quad (8)$$

Where  $f$  is the frequency

$G(f)$  is the output PSD in terms of stress amplitude

The expression above is important in computing the number of cycles  $N(S)$ . Expression for computation is shown in the expression below.

$$N(S) = E(P) * T * p(S) \quad (9)$$

Where  $T$  is the total time considered for fatigue damage computation,  $E(P)$  is the expected number of peaks and  $p(S)$  is the probability of stress range  $S$  computed by using the expression below.

$$E(P) = \sqrt{\frac{m_2}{m_0}} \quad (10)$$

$$P(S) = \frac{\frac{D_1 e^{-Z/Q}}{Q} + \frac{D_2 Z e^{-Z^2/2R^2}}{R^2} + D_3 Z e^{-Z^2/2}}{2\sqrt{m_0}} \quad (11)$$

The constants used in the expression above are computed using the expressions below.

$$x_m = \frac{m_1}{m_0} \sqrt{\frac{m_2}{m_4}} \quad (12)$$

$$y' = \frac{m_2}{\sqrt{m_0 m_4}} \quad (13)$$

$$D_1 = \frac{2(x_m - y'^2)}{1 + y'^2} \quad (14)$$

$$R = \frac{y' - x_m - D_1^2}{1 - y' - D_1 + D_1^2} \quad (15)$$

$$D_2 = \frac{1 - y' - D_1 + D_1^2}{1 - R} \quad (16)$$

$$D_3 = 1 - D_1 - D_2 \quad (17)$$

$$Q = \frac{1.25(y' - D_3 - D_2 - R)}{D_1} \quad (18)$$

$$Z = \frac{S}{2\sqrt{m_0}} \quad (19)$$

In the expressions above  $x_m$  is the mean frequency,  $Z$  refers to the normalized stress range,  $y'$  is the irregularity factor and other parameters refer to constants.

Once all computations required are executed, a plot of various stress ranges ( $S$ ) and the Probability Density Function (PDF) is carried out. The area under the curve gives the fatigue damage,  $D$ . Calculations carried out were on mooring line S3 alone and were executed in MATLAB.



### 3. RESULTS AND DISCUSSION

The Figure 2 below shows the total damage on mooring lines located on the starboard side of the vessel. It reveals a lot of information about which mooring line on the FPSO is more likely to experience a higher amount of damage. Careful observation shows that S4 is more likely to experience a higher amount of damage with S5 and S6 having a similar profile. It is important to note that S4 to S6 are located to the aft of the FPSO. S1 to S3 from the charts is observed to have a lower damage profile on all line segments. Candidates for regular checks would be the S4 to S6. It is important to note that low damage profile doesn't guarantee reliability. In-Plane Bending (IPB) and Out of Plane Bending (OPB) are also known to cause failures in rightly designed chains as a lot of normal bending stresses are introduced.

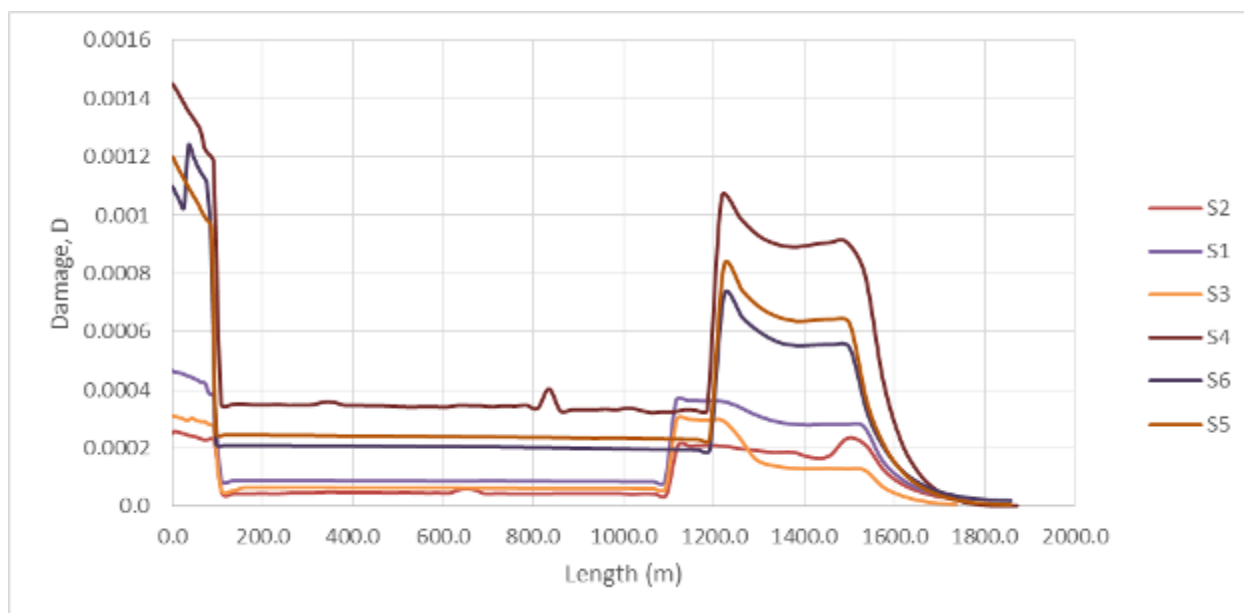


**Figure 2: Total Damage across Mooring Line Lengths (S1-6)**

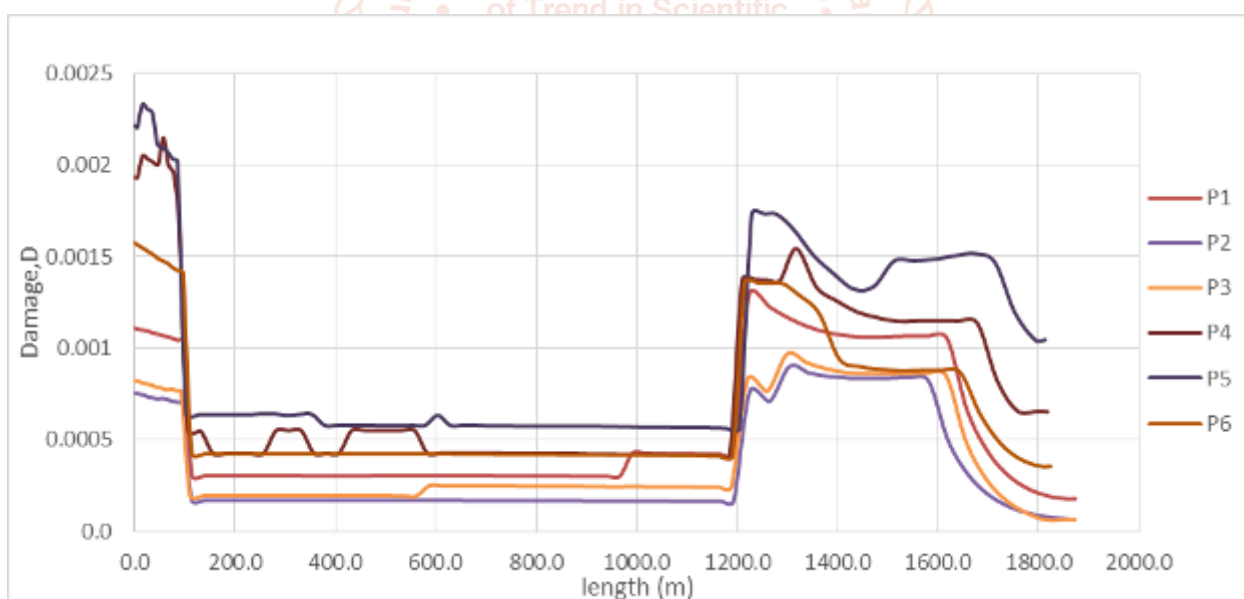


**Figure 3: Total Damage across Mooring Line Lengths (P1-6)**

The damage profile of P1 to P6 as shown in figure 2 above start at higher levels when compared to that of S series. This can be attributed largely to the FPSO orientation and metocean conditions. The impacts of forces induced by LF motions can be attributed to this as well. P5 and P4 have the highest profiles on all sections of the mooring lines and look like damage in the bottom chains are a bit erratic. All mooring lines in the analysis have sections where the damage readings are at 0. Similarities in the damage profile structure is observed because all lines have similar mechanical properties and structural arrangements as seen in the table of the mooring lines segment.

The fatigue life curves of the portside and starboard sides obtained from Orcaflex simulation results is shown in figure 4 and 5 below. Amongst the P series, P2 and P3 have the highest fatigue life owing to their very low

damage profile as seen in the preceding figures. P4 and P5 have the lowest fatigue life in all sections. The S series lines have higher fatigue lives and consequently more likely to last longer than the P series lines.

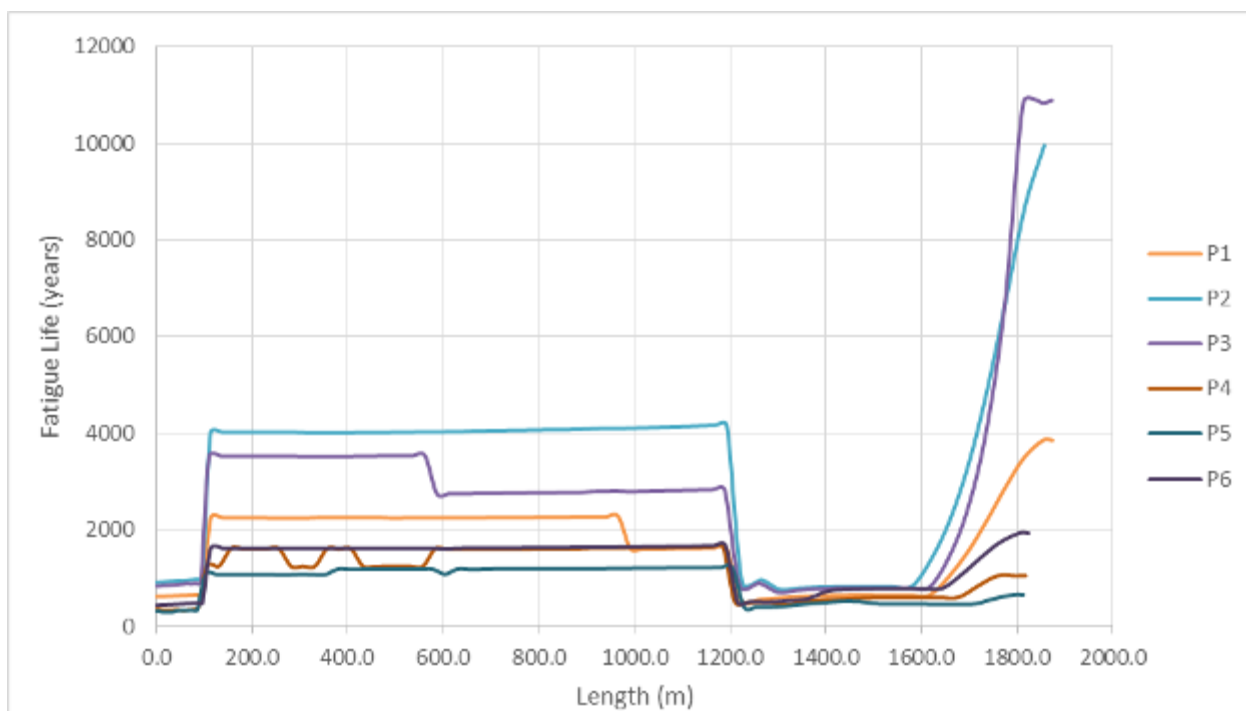


**Figure 4: Fatigue Life across all Mooring Line Lengths (P1-6)**

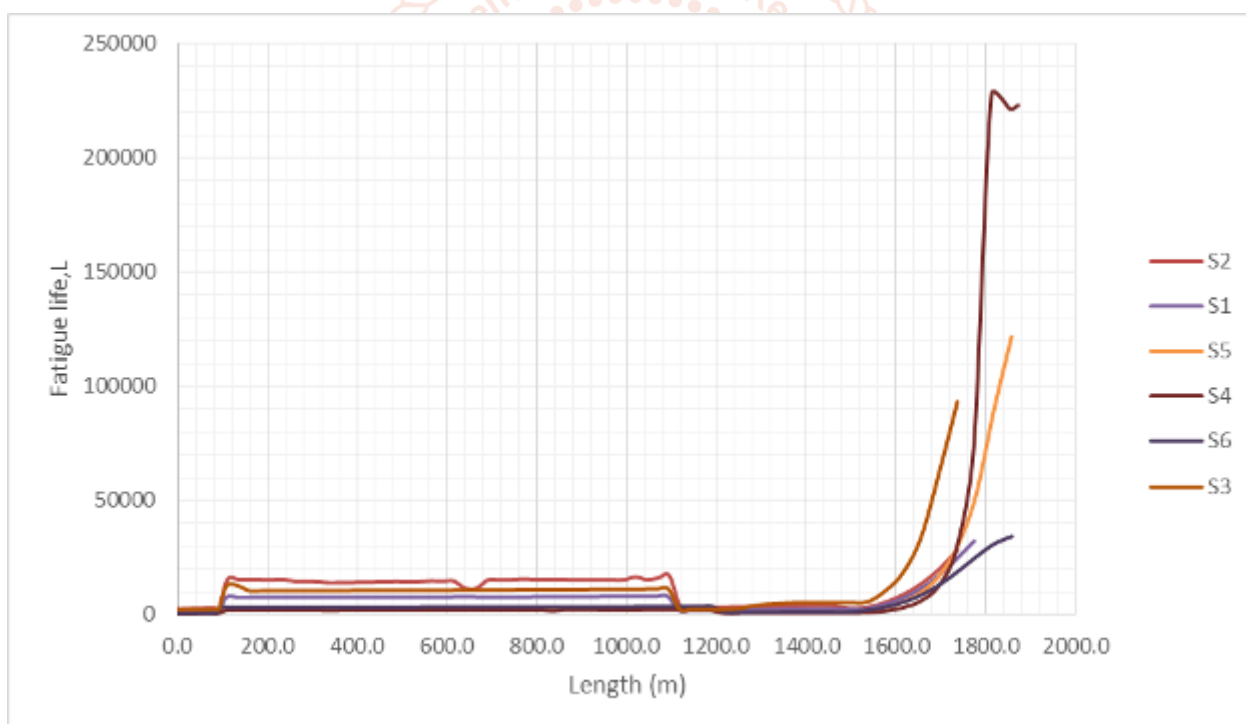


**Figure 5 Fatigue Life across all Mooring Line Lengths (S1-6)**

### 3.2. Frequency Domain Fatigue Analysis

This section addresses the fatigue damage of mooring line S3 at Ends A and B in frequency domain as well as key results obtained from dynamic simulation in Orcaflex. Results obtained from the simulations were used as inputs for Dirlik formula applications and Power Spectral Density (PSD) computations.

Figure 6 below shows the time history of tensions at ends A and B of the mooring line. End A is the point of attachment of the mooring line to the vessel while End B refers to the attachment to the suction pile at touchdown. Simulation history results extracted excluded the build-up stage of the run so extraction starts from time 0 seconds. Time interval of the tensions 0.05 is 0.05 seconds over a duration of 5400 seconds. Total number of data points extracted for each of the plots below is 108,000 points. The spectra obtained after plotting are narrow banded at some point. Time history of End B can be said to be narrow banded for all time durations. However End A is narrow banded from 0 to around 2743 seconds after which the tension range becomes

magnified. This turns the spectrum to a bimodal type. The maximum tension developed in the mooring line at End A is 9362 KN while the least tension developed at this end is 19.66KN. At End B the results are way lesser than End A. The maximum effective tension developed here is 1399KN and the least is 1136 KN. The stress time history is also similar to the tension time history.

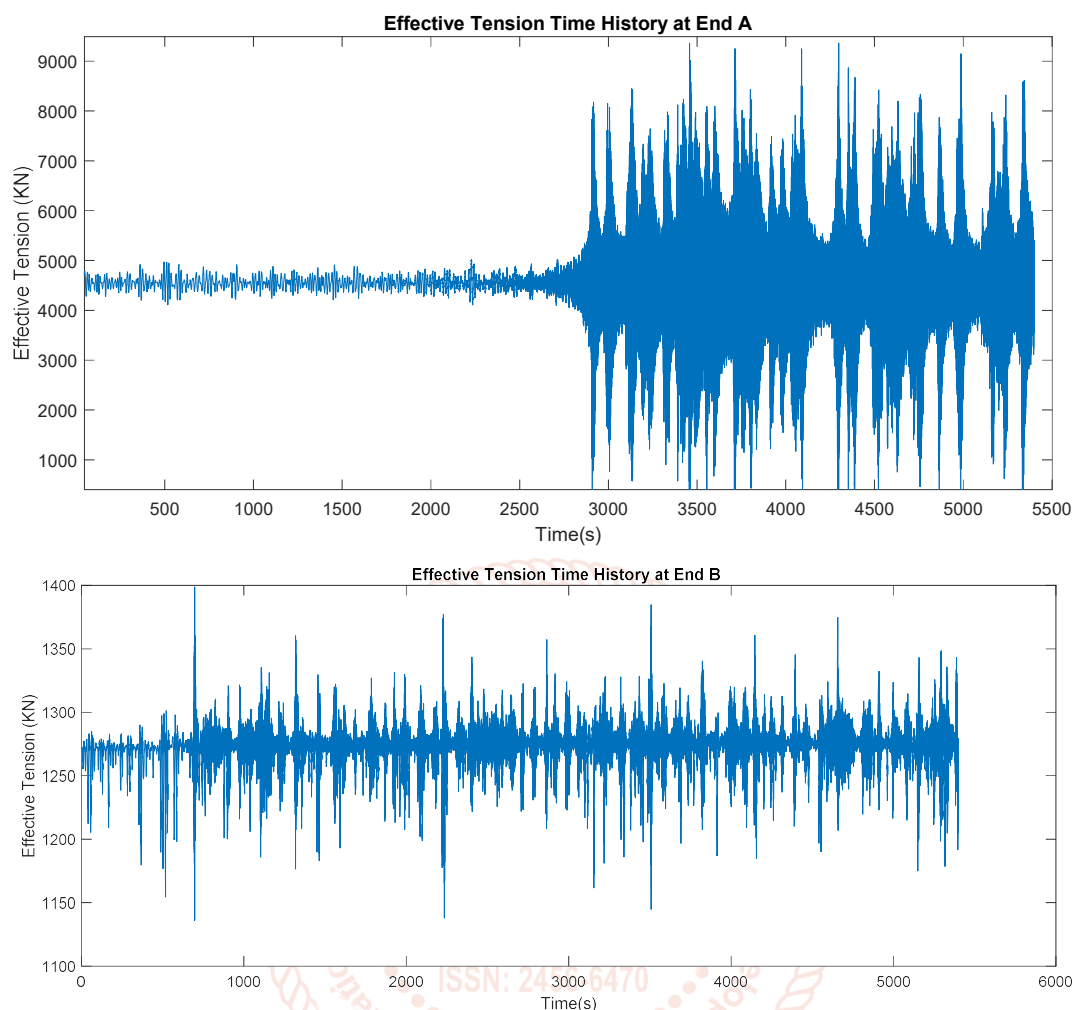


**Figure 6: Tension Time History of Mooring Line at Ends A and B**

Tension cycles can be extracted across all nodes on the mooring lines so closer examination of the variation of tension across all nodes can be closely assessed to identify areas of high tension and for more detailed damage considerations. The stress derivative of the tension cycle above was used as a basis for the computation of the Power Spectral Density (PSD) for ends A and B shown in the figures below.

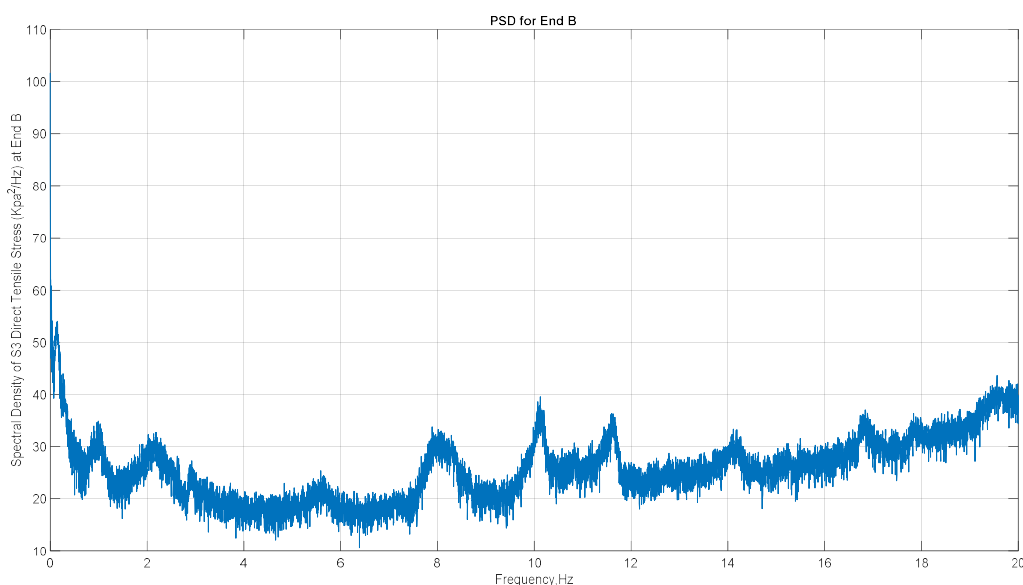


**Figure 7: Power Spectral Density (PSD) for End B**

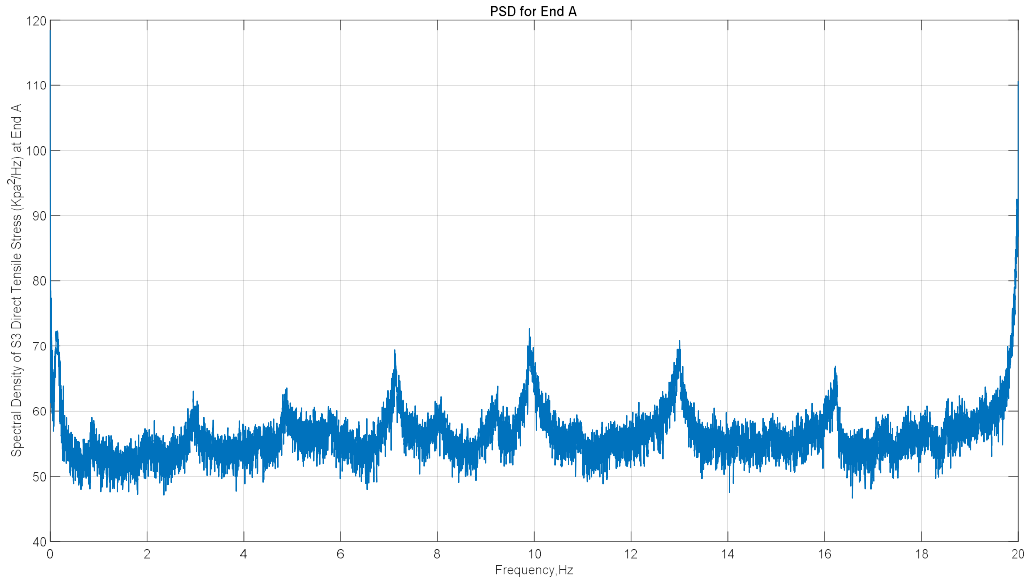


**Figure 8: Power Spectral Density (PSD) for End A**

Power spectral Density (PSD) is an important stage in the computation of fatigue damage in the frequency domain. It shows the impacts or strengths of the tension signals at various frequencies. The peak in the figure indicates areas of interest whose frequencies have been normalized. The region under the PSD curves represents the power of the spectrum.

On completion of computation, using the Dirlik’s method the results of the damage done at an interval of 300 is shown in Table 4.2 below.

**Table 9: Table of Damage obtained using Dirlik’s Method**

Arc Length (m)	Damage
0	7.80E-07
320	1.24E-08
640	1.24E-08
960	7.27E-09
1280	1.01E-07
1600	5.78E-08
1920	5.31E-08

A plot of the results is shown in Figure 9 below. The figure also helps compares the damage results obtained from both methods used in the thesis. Both methods show that the results have similar trajectories and profiles along over 50 percent of the mooring line arc lengths.

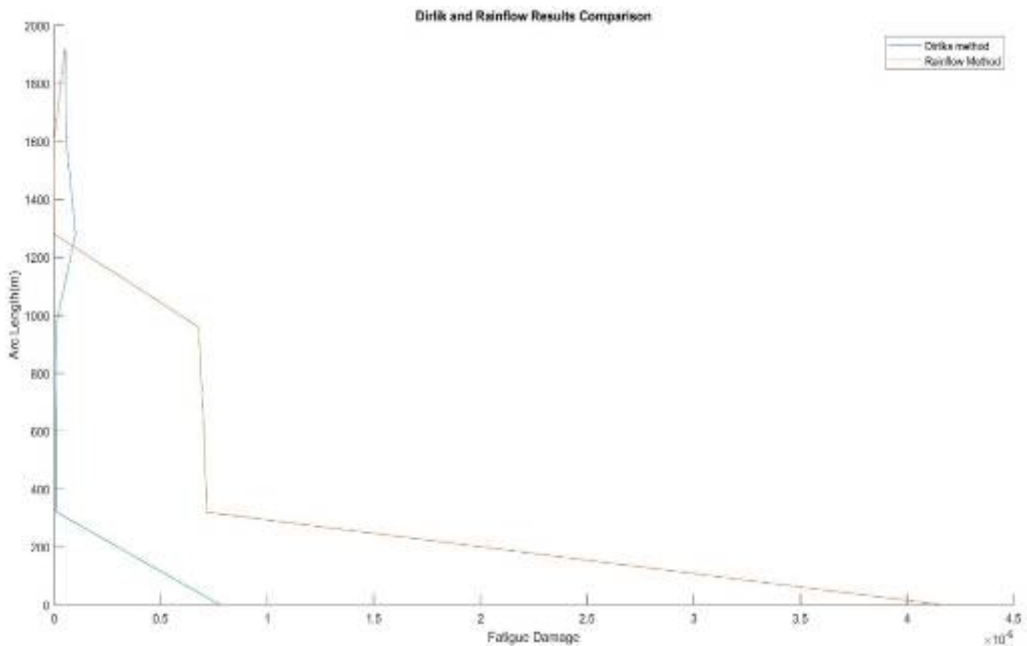


**Figure 9: Results Comparison of Dirlik and Rainflow analysis Results.**



### 3.3. Weibull Analysis Results

Results from this session aims to identify and constrict the range of values that will be recommended. Data used for the plots is shown below for two wave classes. It represents results for the wire rope section. Wave 3 is selected to represent the ULS state the FPSO is being designed to operate in.

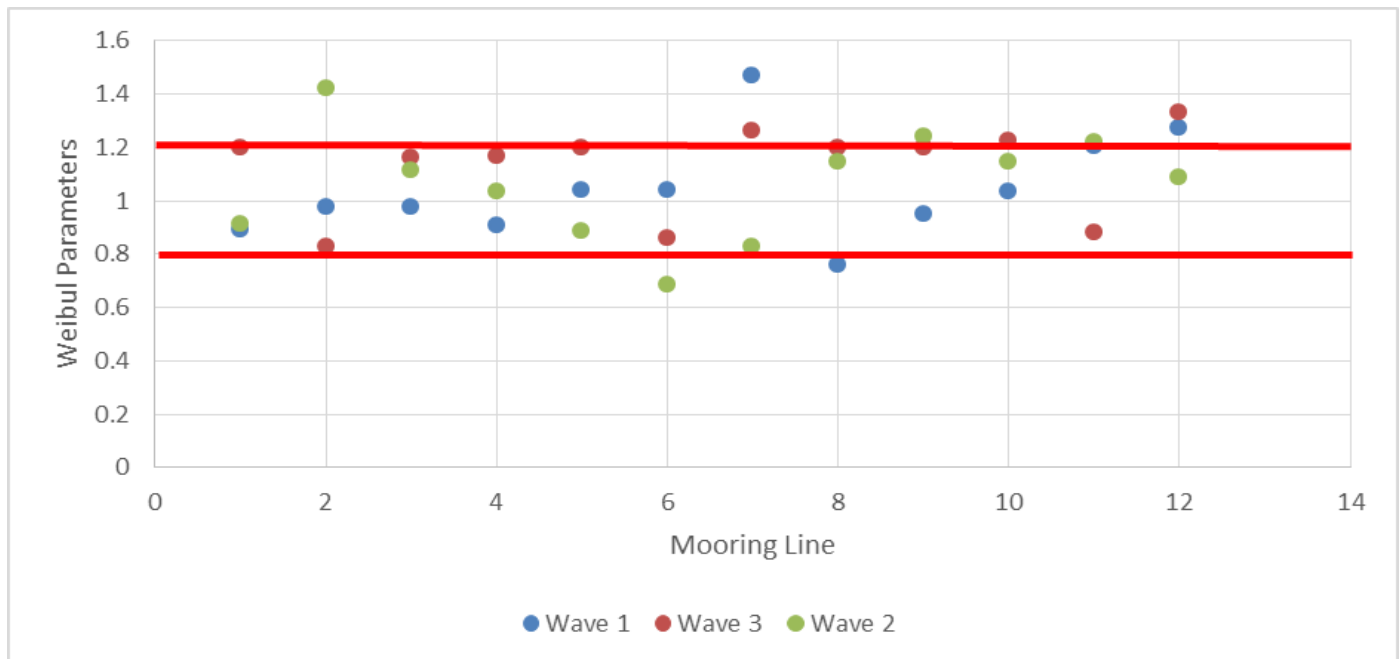


**Figure 10: Average h parameters obtained from analysis.**

Analysis of the results in the previous session helps streamline the possible values of the weibull parameter down to a range between 0.8 and 1.2 marked by the thick lines in the figure.

### 4. CONCLUSION

The research was carried out to analyze fatigue life of mooring lines and come up with a more streamlined Weibull h parameter for analysis in the Gulf of Guinea. The results of the thesis helped streamline the already existing range of h parameters down to a range of 0.4 (0.8 to 1.2) from 1.0(0.5 to 1.5) specified by Weibull in his research. 12 Wave classes were analyzed using LF forces considerations that were specified in the software. For Weibull analysis, simulations were carried out considering WF and LF motions (combined) as well in line with DNV regulations. Some of the inbuilt options in the software that made this possible include applied load, wave load, wave drift load, wave drift damping, added mass damping etc.

The results from Rain flow analysis in orcaflex also showed that all maximum and minimum stresses in all the mooring lines were within the limits of the breaking strengths specified according to DNV OS E301 guidelines. Dirlik's method application also showed the fatigue damage performance over the periods of exposure was very safe. Fatigue life computed showed the mooring lines will be able to last for more than 500 years. However, the analysis was carried out without risers and offtake buoy. As a result, further analysis must be done to access their impacts.

### REFERENCES

- [1] BERGE. (2006). Fatigue and Fracture Design of Marine Structures.
- [2] Chanhoe Kang, C. L. -H. -T. (2016). Fatigue Analysis of Spread Mooring Line. *International Journal of Geological and Environmental Engineering*, 504-510.
- [3] Curtis E. Larsen, T. I. (2014). A review of spectral methods for variable amplitude fatigue prediction and new results. *3rd International Conference on Material and Component Performance under Variable Amplitude Loading, VAL2015* (pp. 243-250). Elsevier.
- [4] K. T. Ma, A. D. (2013). A historical review on integrity issues of permanent mooring system. *Offshore Technology Conference*. Houston.
- [5] Kim Y., K. M. (2017). Nonlinear Finite Element Analysis for Mooring Chain Considering OPB/IPB. *Journal of Ocean Engineering Technology*, 299-307.
- [6] Pankaj Dheer, D. I. (2017). Fatigue assessment of offshore tubular Structures Using Dirlik's Method to Establish the Procedure. *Delft University of Technology*.
- [7] Rampi L., B. A. (2016). Chain Out of Plain Bending (OPB) Fatigue Joint Industry Project

- (JIP) FEA Results and Multiaxiality Study Results. *35th International Conference on Ocean, Offshore and Arctic Engineering*.
- [8] S. DJAKOURÉ, P. P. (2017). Respective Roles of the Guinea Current and Local Winds on the Coastal Upwelling in the Northern Gulf of Guinea. *Journal of Physical Oceanography*, 1367-1387.
- [9] Yooil Kim, M. -S. K. -J. (2018). Fatigue analysis on the mooring chain of a spread moored FPSO considering the OPB and IPB. *International Journal of Naval Architecture and Ocean Engineering*, 178-201.

